JACS
JOURNAL OF THE AMERICAN CHEMICAL SOCIETY

Communication

pubs.acs.org/JACS

Click Quantitative Mass Spectrometry Identifies PIWIL3 as a Mechanistic Target of RNA Interference Activator Enoxacin in Cancer Cells

Nathan S. Abell,[†,#] Marvin Mercado,[†,#] Tatiana Cañeque,[‡,§,⊥,∥] Raphaël Rodriguez,[*,‡,§,⊥,∥] and Blerta Xhemalce[*,†]

[†]Department of Molecular Biosciences, University of Texas at Austin, 2500 Speedway, Austin, Texas 78712, United States
[‡]UPR2301, Institut de Chimie des Substances Naturelles, 1 avenue de la Terrasse, 91198 Gif-sur-Yvette Cedex, France
[§]Organic Synthesis and Cell Biology Group, Institut Curie, PSL Research University, 26 rue d'Ulm, 75248 Paris Cedex 05, France
[⊥]CNRS UMR3666, 75005 Paris, France
[∥]INSERM U1143, 75005 Paris, France

Supporting Information

ABSTRACT: Enoxacin is a small molecule that stimulates RNA interference (RNAi) and acts as a growth inhibitor selectively in cancer but not in untransformed cells. Here, we used alkenox, a clickable enoxacin surrogate, coupled with quantitative mass spectrometry, to identify PIWIL3 as a mechanistic target of enoxacin. PIWIL3 is an Argonaute protein of the PIWI subfamily that is mainly expressed in the germline and that mediates RNAi through piRNAs. Our results suggest that cancer cells re-express PIWIL3 to repress RNAi through miRNAs and thus open a new opportunity for cancer-specific targeting.

Enoxacin is a member of the fluoroquinolone family with a history of clinical use in the treatment of various bacterial infections.[1] Although its anti-infection use has declined in favor of other antibiotics, a resurgence of interest in enoxacin was prompted by its identification in a large-scale small-molecule screen as a booster of RNA interference (RNAi) and microRNA (miRNA) processing in human cells.[2] miRNAs are small, 18−24 nucleotide RNA molecules that post-transcriptionally regulate gene expression. They are transcribed as long primary transcripts (pri-miRNAs) and cleaved in the nucleus by Drosha protein to shorter hairpin precursors (pre-miRNAs). Once exported from the nucleus to the cytosol, pre-miRNAs are processed by Dicer protein to yield a short RNA duplex. One of the strands, called the guide strand, is further loaded into the AGO1−4 Argonaute proteins of the RNA-induced silencing complex (RISC) to regulate the stability or translation of the target messenger RNA (mRNA) by base pairing between the guide strand and the mRNA's 3′ untranslated region.[3] In addition to its endogenous role in regulating gene expression, this pathway is largely exploited by researchers to knock down proteins by RNAi through exogenously supplied siRNA/shRNAs.

The initial small-molecule screen mentioned above demonstrated that enoxacin treatment increases the efficiency of exogenous siRNA- and shRNA-mediated gene silencing.[2,4] Additional experiments also revealed increases in endogenous miRNA levels and rates of miRNA-RISC loading.[2,5,6] Importantly, enoxacin strongly inhibits growth and colony formation in various cancer cell lines, increases their rate of apoptosis, and reduces primary tumor xenograft growth in nude mice.[5,6] Notably, the anti-proliferative properties of enoxacin are specific to cancer cells, as both non-transformed cell lines and primary cells are refractory to enoxacin treatment.[5]

The miRNA processing stimulatory properties of enoxacin have been attributed to its binding to TRBP, a Dicer cofactor.[5] However, a separate study showed an absence of correlation between the effect of enoxacin on miRNA levels and TRBP expression levels.[6] Moreover, knockout of TARBP2, the gene encoding TRBP, in the human HeLa cell line displayed no effect on Dicer stability, miRNA abundance, or Argonaute loading compared to the parental cell line,[7] suggesting that the relationship between the microRNA pathway and enoxacin may be more intricate than anticipated. In addition, the molecular mechanisms underlying the cancer-specific activity of enoxacin are not known and warrant further study.

To this end, we sought to engineer a molecular probe to detect and purify putative targets of enoxacin by bio-orthogonal chemical ligation.[8−12] We first synthesized an alkyne-containing enoxacin derivative that we named alkenox (Figure 1A). We introduced the alkyne onto the piperazine moiety. The compound was conveniently synthesized in one step from commercially available enoxacin by means of a chemoselective alkylation in the presence of propargyl chloride and sodium carbonate (Supporting Information (SI), including Figures S1 and S2). In order to determine whether alkenox retained the biological properties of enoxacin, we treated MCF7 breast cancer cells with alkenox in parallel to unmodified enoxacin and carrier. We measured their effect on cell proliferation with a MTT colorimetric assay assessing cell metabolic activity (SI). As shown in Figure S3, enoxacin strongly inhibited cell growth, with a calculated IC_{50} (the concentration of drug required to inhibit cell growth by 50% compared to the carrier) value of 124.2 μM, comparable to the results previously published by

Received: November 15, 2016
Published: January 17, 2017

DOI: 10.1021/jacs.6b11751
J. Am. Chem. Soc. 2017, 139, 1400−1403

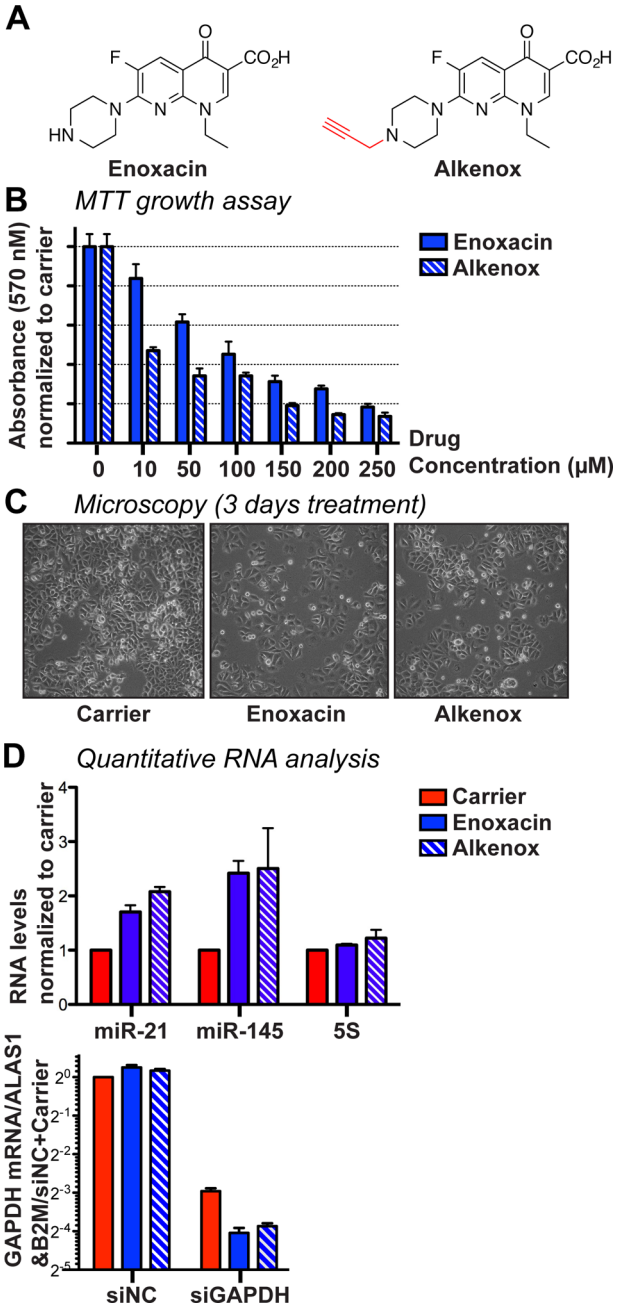

Figure 1. (A) Molecular structure of enoxacin and its alkyne-containing derivative, alkenox. (B) MTT proliferation assays in MCF7 cells treated with enoxacin and alkenox (5-day regimen). Shown are means ± SD relative to carrier. (C) Bright-field microscopy images of MCF7 cells treated with 125 μM enoxacin, alkenox, or carrier (3-day regimen). (D) Left: RT-qPCR analysis of miR-21, miR-145, and the control 5S rRNA from MCF7 cells treated as in (C). Shown are means ± SEM, after normalization to the carrier-treated cells. Right: RT-qPCR analysis of GAPDH mRNA in MCF7-siNC and siGAPDH cells treated with 100 μM enoxacin, alkenox, or carrier (24 h). Shown are averages ± SEM, after normalization to ALAS1, B2M, and siNC +carrier.

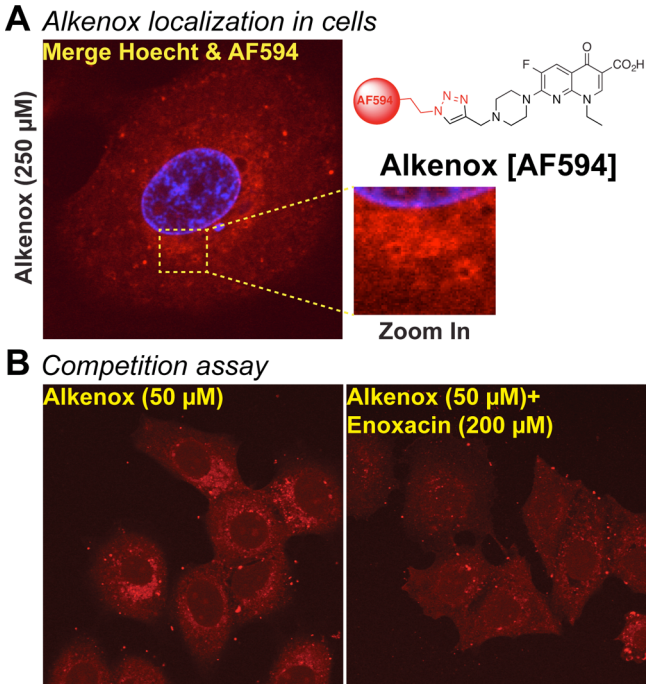

Figure 2. (A) Image of a representative alkenox-treated MCF7 cell labeled with AF-594 post-treatment (see also Figure S4). (B) Image showing alkenox [AF-594] in MCF7 cells treated with 50 μM alkenox and carrier or 200 μM enoxacin (see also Figure S5).

Melo et al.[5] Under the same conditions, alkenox reproducibly showed a similar though more pronounced effect on cellular proliferation compared to enoxacin, especially at the lower doses of the drug (Figure 1B,C). Given that enoxacin activates the miRNA processing pathway, we next measured the levels of mature miR-21 and miR-145 in MCF7 cells treated with alkenox, as previously described.[13] Figure 1D shows that alkenox treatment increases the levels of mature miRNAs, consistent with the previously described effect of enoxacin.[2,5] Alkenox also enhances the efficiency of siRNA-mediated knockdown similarly to enoxacin (Figure 1D). Together, our data suggest that alkenox mimics the effects of enoxacin with regard to both inhibition of cell proliferation and stimulation of the si/miRNA pathway.

We next sought to determine the cellular localization of enoxacin. We used a copper(II)-catalyzed click reaction to covalently attach an azide-conjugated Alexa Fluor 594 fluorophore to alkenox in MCF7 cells, followed by confocal fluorescence microscopy. Cells treated with carrier or regular enoxacin without the alkyne group (Figure S4B) were used as negative controls. The basal background from these cells was very low under our extensively optimized conditions (SI). Importantly, we observed a distinct signal from the alkenox-treated cells (Figure S4), showing that the alkyne group of alkenox is accessible and reactive within cells. Consistent with the effect of enoxacin on the RNAi pathway, alkenox was mainly cytoplasmic, with a clearly outlined nuclear−cytoplasmic boundary (Figure S4C). Alkenox staining was not uniform, with its levels being highest in the regions juxtaposed to the nucleus (Figures 2A and S4D) and defining spherical structures (zoom-in, Figure 2A). Furthermore, excess enoxacin significantly reduced alkenox staining, suggesting that alkenox and enoxacin compete for the same target(s) (Figures 2B and S5).

We next localized alkenox in HeLa cells in which both copies of TARBP2 gene encoding TRBP were inactivated by zinc finger nuclease technology.[7] Alkenox staining did not change in two independent TRBP knockout clones compared to their parental cells (Figure S6), suggesting that TRBP may not be the sole target of enoxacin. Supporting this finding, both TRBP

DOI: 10.1021/jacs.6b11751
J. Am. Chem. Soc. 2017, 139, 1400−1403

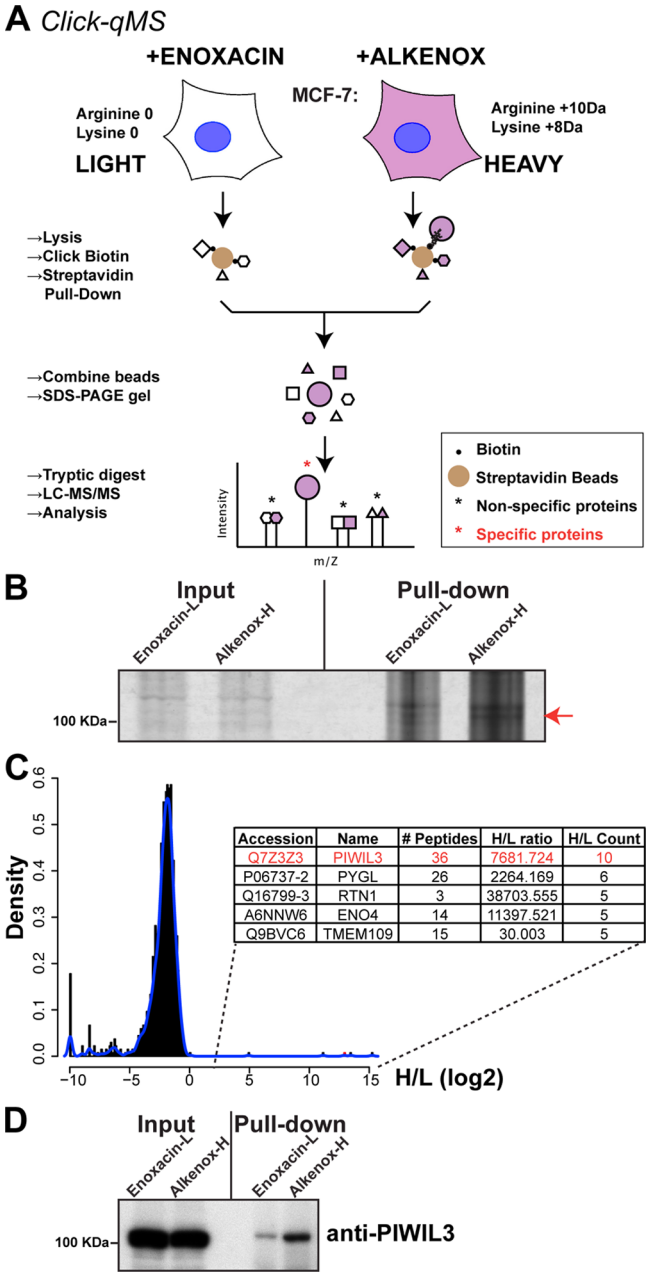

Figure 3. (A) Click-qMS experimental design (see SI for details). (B) Silver-stained gel of inputs and pull-downs. Red arrow points to the alkenox-specific band. (C) Click-qMS results showing distribution of the 1364 proteins with H/L counts ≥5 (H/L ratio (log 2) on *x*-axis, density on *y*-axis); histogram overlaid with density curve is shown in blue. Table shows proteins with H/L ≥ 2 (see Table S2 for the complete list). (D) Western blot with a PIWIL3 antibody of Click-qMS input and pull-downs.

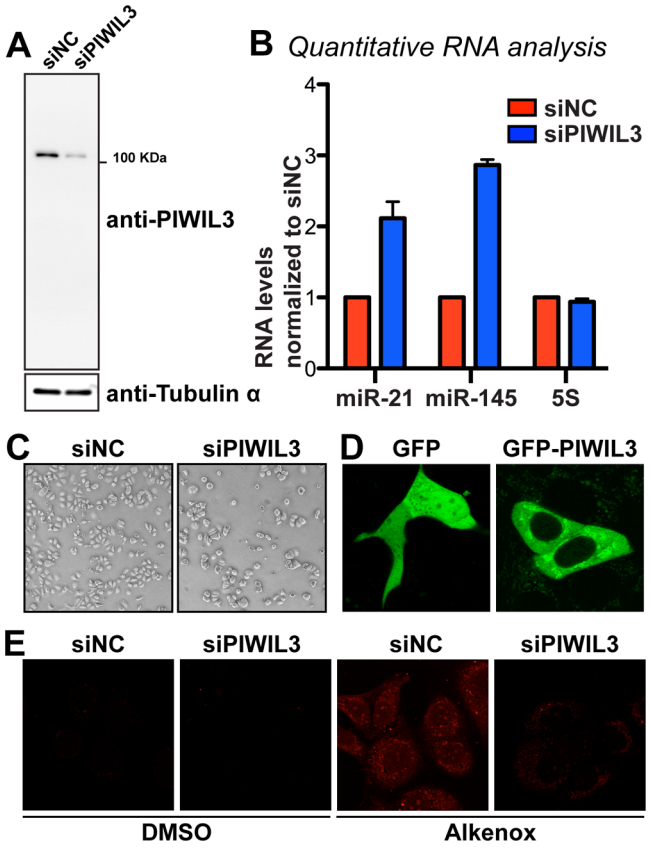

Figure 4. (A) Western blot analysis of MCF7 cells transfected with siNC or siPIWIL3. (B) RT-qPCR analysis as in Figure 1D. (C) Bright-field microscopy of MCF7 cells transfected with siNC and siPIWIL3. (D) Live confocal microscopy of MCF-7 cells expressing GFP or GFP-PIWIL3 for 24 h. (E) Confocal fluorescence microscopy as in Figure 2A.

knockout clones were as sensitive to enoxacin as their parental cells (Figure S7).

To determine the target(s) of enoxacin, we developed a Click-qMS method that combines alkenox click pull-downs from treated cells with quantitative mass spectrometry. This method is different from classical affinity purification mass spectrometry (AP-MS) methods that use drugs coupled to beads to pull down proteins from untreated cellular lysates.[14] In our method, MCF7 cells were treated with enoxacin or alkenox, lysed in Click-iT buffer, clicked to a biotin-azide, and pulled down with streptavidin beads (Figure 3A and SI). To eliminate the high background from biotinylated cellular proteins or proteins that bind to beads, we performed SILAC (stable isotope labeling with amino acids in cell culture")[15] (Figure 3A and SI). Specifically, we treated MCF7 cells grown in "light" media with enoxacin, and cells grown in "heavy" media with alkenox. In this combination, the proteins pulled down by alkenox should have a heavy/light (H/L) ratio significantly superior to 1. An initial SDS-PAGE and silver stain analysis of these pull-downs showed a specific band migrating just above 100 kDa, indicated by a red arrow in Figure 3B. Further LC-MS/MS analysis of the pooled pull-downs identified a total of 4240 proteins, of which 1364 had at least five measurable heavy/light counts (H/L counts ≥5) (Table S2). The vast majority of these proteins were not enriched in alkenox versus enoxacin pull-downs, and only five proteins showed a H/L ratio >2 (Figure 3C and Table S2). Among these, the protein with the highest number of peptides and H/L counts, an H/L ratio of ∼7500, and the expected size of ∼100 kDa was PIWIL3 (Figures 3C and S8). Western blot with a specific anti-PIWIL3 antibody of the pull-down inputs verified that PIWIL3 protein levels were not affected by growth in "heavy" medium (Figure 3D). Importantly, this Western blot validated by an independent means the results of our Click-qMS analysis that PIWIL3 is specifically enriched in the alkenox pull-downs (Figure 3D).

DOI: 10.1021/jacs.6b11751
J. Am. Chem. Soc. 2017, 139, 1400−1403

PIWIL3 is an Argonaute protein of the PIWI subfamily that is typically testis specific.[16] However, as shown by our Click-qMS results and Figure 4A, PIWIL3 is expressed in the breast cancer MCF7 cells. While few data sets contain probes for PIWIL3 mRNA expression, specific antibodies against PIWIL3 have been raised and have shown increased expression of PIWIL3 protein in tumors compared to normal tissue in ovarian, colon, and gastric cancer.[17−19] We next checked the effects of depleting PIWIL3 in MCF7 cells (Figure 4A). Knock-down of PIWIL3 increased miRNA levels (Figure 4A,B) and induced a growth defect (Figures 4C and S9) similar to enoxacin treatment. Interestingly, GFP-tagged PIWIL3 also showed cytoplasmic localization, where it defined spherical substructures that were reminiscent of those defined by alkenox (Figure 4D). Finally, the staining of alkenox was severely reduced in cells depleted for PIWIL3 (Figure 4E), further validating PIWIL3 as a mechanistic target of enoxacin.

Overall, given that siRNA depletion of PIWIL3 mimics the effect of enoxacin, enoxacin treatment likely results in a loss of PIWIL3 activity. Thus, through an unbiased approach using a clickable drug derivative and quantitative mass spectrometry, we discovered one of the primary mechanistic targets of enoxacin as PIWIL3, a member of the PIWI subclade of Argonaute proteins that mediate RNAi. Our findings suggest that re-expression of proteins of the piRNA pathway in cancer cells may repress the miRNA pathway to promote cancer cell growth. Moreover, our finding explains enoxacin's specificity to cancer cells: PIWIL3 is expressed in various cancers,[17−19] but is limited to testis in normal tissues.[16] This opens exciting avenues for the targeting of the piRNA pathway in cancer.

■ ASSOCIATED CONTENT

Supporting Information

The Supporting Information is available free of charge on the ACS Publications website at DOI: 10.1021/jacs.6b11751.

Experimental procedures and supplementary data, including Figures S1−S9 and Table S1 (PDF)

Table S2, listing 1364 proteins with H/L counts ≥5 (XLSX)

■ AUTHOR INFORMATION

Corresponding Authors

*raphael.rodriguez@curie.fr

*b.xhemalce@austin.utexas.edu

ORCID

Tatiana Cañeque: 0000-0002-1110-0643

Blerta Xhemalce: 0000-0002-0517-9607

Author Contributions

#N.S.A. and M.M. contributed equally.

Notes

The authors declare no competing financial interest.

■ ACKNOWLEDGMENTS

The Q-Exactive Mass Spectrometer in the Xhemalce lab was in part supported by the Institute of Cellular and Molecular Biology at the University of Texas at Austin. This work was supported by funds to B.X. from the College of Natural Sciences and the Institute of Cellular and Molecular Biology at the University of Texas at Austin, the Welch Foundation F1859 and the Department of Defense - Congressionally Directed Medical Research Programs - Breast Cancer Research Program - Breakthrough Award W81XWH-16-1-0352. We would like to particularly thank Dr. Helene Ipas in the Xhemalce lab for valuable technical assistance. We also thank Dr. Kyle Miller (UT Austin) for the use of his lab's confocal microscope, Dr. Marvin Whiteley (UT Austin) for the use of his lab's plate reader and Dr. Fade Gong in the Miller lab for help with setting up live microscopy. Alkenox design and synthesis was supported by funds to R.R. from the European Research Council 647973, Fondation pour la Recherche Medicale AJE20141031486, Emergence Ville de Paris and La Ligue Contre le Cancer. We would like to thank CNRS (Centre National pour la Recherche Scientifique) for funding T.C. and R.R.

■ REFERENCES

(1) Schaeffer, A. J. *Am. J. Med.* **2002**, *113*, 45S.

(2) Shan, G.; Li, Y.; Zhang, J.; Li, W.; Szulwach, K. E.; Duan, R.; Faghihi, M. A.; Khalil, A. M.; Lu, L.; Paroo, Z.; Chan, A. W.; Shi, Z.; Liu, Q.; Wahlestedt, C.; He, C.; Jin, P. *Nat. Biotechnol.* **2008**, *26*, 933.

(3) Ha, M.; Kim, V. N. *Nat. Rev. Mol. Cell Biol.* **2014**, *15*, 509.

(4) Zhang, Q.; Zhang, C.; Xi, Z. *Cell Res.* **2008**, *18*, 1077.

(5) Melo, S.; Villanueva, A.; Moutinho, C.; Davalos, V.; Spizzo, R.; Ivan, C.; Rossi, S.; Setien, F.; Casanovas, O.; Simo-Riudalbas, L.; Carmona, J.; Carrere, J.; Vidal, A.; Aytes, A.; Puertas, S.; Ropero, S.; Kalluri, R.; Croce, C. M.; Calin, G. A.; Esteller, M. *Proc. Natl. Acad. Sci. U. S. A.* **2011**, *108*, 4394.

(6) Sousa, E.; Graca, I.; Baptista, T.; Vieira, F. Q.; Palmeira, C.; Henrique, R.; Jeronimo, C. *Epigenetics* **2013**, *8*, 548.

(7) Kim, Y.; Yeo, J.; Lee, J. H.; Cho, J.; Seo, D.; Kim, J. S.; Kim, V. N. *Cell Rep.* **2014**, *9*, 1061.

(8) Kolb, H. C.; Finn, M. G.; Sharpless, K. B. *Angew. Chem., Int. Ed.* **2001**, *40*, 2004.

(9) Larrieu, D.; Britton, S.; Demir, M.; Rodriguez, R.; Jackson, S. P. *Science* **2014**, *344*, 527.

(10) Rodriguez, R.; Miller, K. M. *Nat. Rev. Genet.* **2014**, *15*, 783.

(11) Rodriguez, R.; Miller, K. M.; Forment, J. V.; Bradshaw, C. R.; Nikan, M.; Britton, S.; Oelschlaegel, T.; Xhemalce, B.; Balasubramanian, S.; Jackson, S. P. *Nat. Chem. Biol.* **2012**, *8*, 301.

(12) Rostovtsev, V. V.; Green, L. G.; Fokin, V. V.; Sharpless, K. B. *Angew. Chem., Int. Ed.* **2002**, *41*, 2596.

(13) Xhemalce, B.; Robson, S. C.; Kouzarides, T. *Cell* **2012**, *151*, 278.

(14) Ong, S. E.; Schenone, M.; Margolin, A. A.; Li, X.; Do, K.; Doud, M. K.; Mani, D. R.; Kuai, L.; Wang, X.; Wood, J. L.; Tolliday, N. J.; Koehler, A. N.; Marcaurelle, L. A.; Golub, T. R.; Gould, R. J.; Schreiber, S. L.; Carr, S. A. *Proc. Natl. Acad. Sci. U. S. A.* **2009**, *106*, 4617.

(15) Bartke, T.; Vermeulen, M.; Xhemalce, B.; Robson, S. C.; Mann, M.; Kouzarides, T. *Cell* **2010**, *143*, 470.

(16) Sasaki, T.; Shiohama, A.; Minoshima, S.; Shimizu, N. *Genomics* **2003**, *82*, 323.

(17) Li, L.; Yu, C.; Gao, H.; Li, Y. *BMC Cancer* **2010**, *10*, 38.

(18) Chen, C.; Liu, J.; Xu, G. *Cancer Biomark.* **2013**, *13*, 315.

(19) Wang, Y.; Liu, Y.; Shen, X.; Zhang, X.; Chen, X.; Yang, C.; Gao, H. *Int. J. Clin. Exp. Pathol.* **2012**, *5*, 315.

DOI: 10.1021/jacs.6b11751
J. Am. Chem. Soc. 2017, 139, 1400−1403